Transformations preceding amorphization in Cr-Ti and Cr-Ti-Fe β phases

Ch. Wirz and A. Blatter

Institute of Applied Physics, University of Berne, CH-3012 Berne, Switzerland

N. Baltzer and M. von Allmen

Cendres et Métaux SA, CH-2501 Bienne, Switzerland

The nonequilibrium bcc solid solutions of Cr-Ti and Cr-Ti-Fe, obtained by quenching bulk material at a moderate cooling rate, undergo partial solid-state amorphization during annealing at a relatively low temperature in the spinodal range. Cyclic and isothermal measurements of the specific heats, the coefficients of thermal expansion, and the resistivities, as well as x-ray diffraction, were performed to examine the vitrification reactions and the configurations involved. The data reveal that vitrification involves a sequence of events led by an exothermic reaction that appears to be displacive in nature. The resulting structure, although crystalline by configuration, displays characteristic features of amorphous materials such as a "glass transition." Configurational amorphization only occurs gradually at temperatures above the glass transition.

I. INTRODUCTION

It is well known that metallic β-phase (bcc) alloys tend to show soft transverse phonon modes indicating a weak restoring force, i.e., a poor mechanical stability.[1] Associated with such modes is a large vibrational entropy. In a number of systems β phases exist only at high temperature, stabilized by the large vibrational entropy contribution to the free energy but become susceptible to displacive transformations (e.g., martensitic) at lower temperature.[2] In a series of publications we have demonstrated that a number of Ti- and Nb-based β-phase transition-metal alloys even undergo spontaneous vitrification upon low-temperature annealing.[3-6]

In Cr-Ti and Cr-Ti-Fe alloys the β solid solution can be retained in bulk form over an extended composition range by quenching at moderate cooling rate. Recent investigations of vitrification in these alloys showed the process to consist of several steps.[7] In particular, elastic effects were found to precede structural disordering. In the present paper we report on more detailed experiments carried out with bulk Cr-Ti and Cr-Ti-Fe alloys in order to characterize the various reactions involved in spontaneous vitrification, as well as the intermediate product phases.

II. EXPERIMENTAL TECHNIQUES

High-purity elemental powders of Cr, Ti, and Fe with ratios Cr_xTi_{100-x} ($x = 20-50$ at. %) and $Cr_{32}Fe_8Ti_{60}$ were first melted and homogenized in an arc-melting system. The melt was then pressure cast into water-cooled copper crucibles to form rods of diameter 2 or 3 mm and length 4–6 cm. The cooling rate achieved—of the order 10^3 K/s—was sufficient to freeze the alloys in their high-temperature β-phase configuration. Water quenched (10^3 K/s) and splat cooled (10^6 K/s) β-$Cr_{40}Ti_{60}$ samples were also prepared for comparison.

Calorimetry, dilatometry, and resistivity measurements under cyclic and isothermal annealing conditions were then performed with these materials. The structure of the samples was checked before and after each processing step by x-ray diffractometry using Cu $K\alpha_1$ radiation.

A Perkin Elmer DSC-4 (DSC denotes differential scanning calorimetry) system combined with a Tads 3600 thermal analysis station was used to determine reaction enthalpies and specific heats between 50 and 600 °C. Sample weights of about 40 mg and heating and cooling rates between 5 and 50 K/min were employed. The temperatures for subsequent isothermal experiments were chosen according to the occurrence of heat effects during a first DSC scan. Temperature and power calibration was carried out using the melting points and heats of fusion of indium and zinc. High-purity argon served as a purge gas. A reference curve, obtained by heating empty pans under identical conditions, was taken for each measurement and subtracted to suppress base-line drifts. The resolution of the DSC system was better than 0.5 J/(mol K).

A Netzsch Type 402E push-rod dilatometer served to monitor changes in the length of the rods. Measurements were conducted in vacuum. Heating rates were kept low (5 K/min) in order to ensure equal temperatures of thermocouple and sample. Isothermal analysis was performed at the same temperatures as with the DSC. The practical resolution of the dilatometer was 50 nm.

The dc resistance of the rods was monitored in a high-vacuum tube furnace using a specially designed high-temperature four-point probe. Processing parameters were the same as used in the dilatometer.

III. EXPERIMENTAL RESULTS

Typical DSC traces obtained from an as-quenched β-$Cr_{40}Ti_{60}$ sample are shown in Fig. 1. During the first heating cycle [Fig. 1(a)] an exothermic reaction occurs

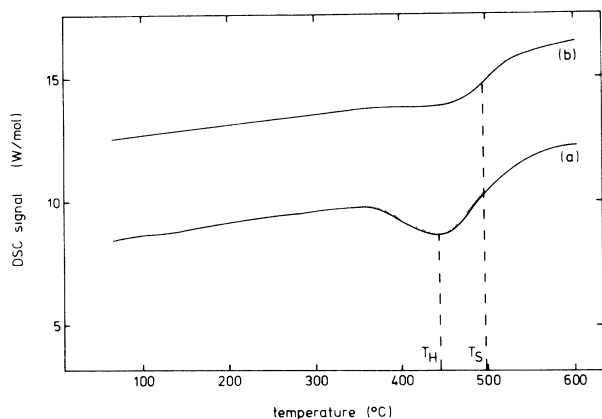FIG. 1. DSC signal vs temperature curves for β-$Cr_{40}Ti_{60}$ obtained at a heating rate of 20 K/min. Trace (a) is from the first and trace (b) from the second heating cycle. (b) has been shifted upwards for the sake of clarity. During the first cycle an exothermic reaction with enthalpy ΔH (shaded area) occurs near T_H. At temperature T_S there is a reversible step.

with the maximum rate at temperature T_H and a total reaction enthalpy ΔH. This reaction (to which we will refer as "enthalpy reaction") is followed by a steplike increase of the specific heat (which we will call "specific-heat reaction") centered at temperature T_S. While the enthalpy reaction is irreversible and has normally completed after the first run, the specific-heat reaction recurs reversibly during successive heating and cooling cycles. This is reflected by the DSC signal from the second heating cycle of the same sample [Fig. 1(b)].

The dilatometer traces from an equivalent sample closely resemble the DSC traces, as is evident from Fig. 2. The apparent thermal expansion coefficient $\alpha = (1/L)(dL/dT)$ first increases slightly with temperature up to about 330 °C and then shows an irreversible depression indicating a decrease of volume, ΔV. The depression is again followed by a reversible step, $\Delta \alpha$. The effects in the dilatometer are seen to occur at a slightly lower temperature than in the DSC, due to the lower heating rate.
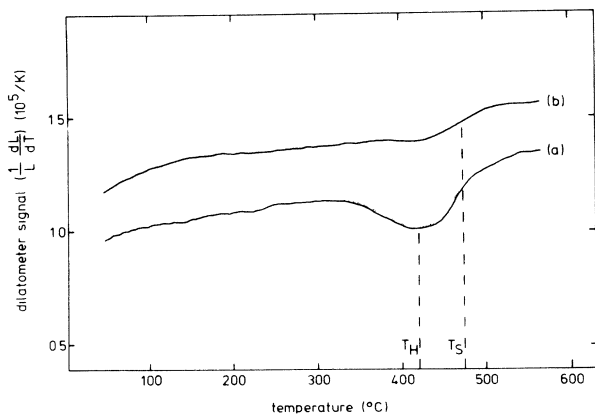

FIG. 2. Dilatometer signal $(1/L)(dL/dT)$ vs temperature curves, analogous to Fig. 1 but with a heating rate of 5 K/min. The shaded area corresponds to a volume contraction ΔV.

The observed process temperatures T_H and T_S, enthalpy and volume changes ΔH and ΔV, and step heights Δc_p and $\Delta \alpha$ for the compositions investigated are given in Table I. T_H and T_S increase with increasing Cr content, and so do ΔH and ΔV (the values at 50 at. % are less reliable). The step heights $\Delta \alpha$ and Δc_p show virtually no concentration dependence. The results for the ternary $Cr_{32}Fe_8Ti_{60}$ alloy are similar to those of $Cr_{40}Ti_{60}$, except that all effects are somewhat larger.

The observed values of ΔH and ΔV depend not only on concentration, but also on the preparation history.[8] No dependence on the preparation method was found, however, for the step heights.

The data of Table I invite some immediate comments. First, the ratio $\Delta H/\Delta V$, included in the last column, may be related to the bulk modulus B. The literature value of B for β-$Cr_{30}Ti_{70}$ is 100 GPa,[9] and that for $Cr_{50}Ti_{50}$ is 147 GPa.[10] For β-$Cr_{40}Ti_{60}$ a value between 85 and 110 GPa was estimated. The agreement with $\Delta H/\Delta V$ is very good, indicating that the Grüneisen factor γ is of order unity.

As for the step heights Δc_p and $\Delta \alpha$, it turns out that their relative magnitudes ($\Delta c_p/c_p$ and $\Delta \alpha/\alpha$) near T_S are about the same (between 0.14 and 0.17), irrespective of the composition. This means that the Grüneisen relation (with molar volume V_{mol})

$$\alpha/c_p = \gamma/(3BV_{mol})$$ (1)

is satisfied for the specific-heat reaction with a constant right-hand side. Given that γ for β-Cr-Ti is of order unity, Eq. (1) again yields bulk moduli B of the order of $\Delta H/\Delta V$. That is, for $Cr_{40}Ti_{60}$ the ratio α/c_p is 4.18×10^{-7} J(m^{-3}) near T_S. Inserting a molar volume of 8.87×10^{-6} m^3/mol (the sum of the concentration weighted partial molar volumes of Cr and Ti) gives a bulk modulus B of 90 GPa.

The development of resistivity of a freshly prepared β-$Cr_{40}Ti_{60}$ rod on heating and subsequent cooling is depicted in Fig. 3. The apparent temperature coefficient of resistivity (TCR), which is the slope of the curve, decreases substantially and abruptly (from 2.5×10^{-4} to 0.1×10^{-4} K^{-1}) at 435 °C, i.e., concomitant with the enthalpy reaction. The decrease is missing in $Cr_{20}Ti_{80}$, which also lacks the enthalpy reaction. As for the specific-heat reaction, it obviously leaves no trace in the resistivity nor in the TCR for any composition. The marked increase of TCR above 700 ° C is due to formation of equilibrium phases (with a TCR of 7.7×10^{-4} K^{-1}). The mentioned TCR values compare well with published thin film data of the β, the vitrified, and the equilibrium phases, respectively.[11,12] The values extrapolated to room temperature yield, as expected, an inverse relationship between resistivity and TCR.[13]

To supplement the information from the scanning measurements, we also carried out isothermal measurements at various temperatures. Results obtained near T_H are summarized in Fig. 4. Calorimetry [(a)] does not reveal anything new. Dilatometry, on the other hand, shows that the initial contraction in the Cr-Ti alloys (but not in Cr-Ti-Fe) is followed by a much larger contraction ex-

TABLE I. Summary of scanning calorimetry (20 K/s) and dilatometry (5 K/s) results. ΔH and ΔV are, respectively, the enthalpy and the volume contraction during the enthalpy reaction at temperature T_H. Δc_p and $\Delta \alpha$ are, respectively, the reversible steps in specific heat and thermal expansion coefficient observed at temperature T_S (the temperatures quoted are those from the calorimeter traces). The last column gives the ratio $\Delta H / \Delta V$. The errors indicated are mainly due to data scattering from sample to sample. The values for $Cr_{50}Ti_{50}$ should be taken as rough approximations, as no pure β phase of this composition could be prepared.

	T_H (°C)	ΔH (J/mol)	ΔV (10^{-4} cm^3/mol)	T_S (°C)	ΔC_p (J/mol K)	$\Delta \alpha$ (10^{-6}/K)	$\Delta H / \Delta V$ (GPa)
$Cr_{20}Ti_{80}$		0 ± 5	0 ± 5	390 ± 5	5.5 ± 0.8	1.4 ± 0.2	
$Cr_{30}Ti_{70}$	370 ± 5	110 ± 10	12 ± 5	420 ± 5	5.2 ± 0.5	1.7 ± 0.3	92
$Cr_{40}Ti_{60}$	440 ± 5	320 ± 30	35 ± 5	495 ± 5	5.0 ± 0.6	2.0 ± 0.4	91
$Cr_{50}Ti_{50}$	490 ± 5	(390)	(21)	535 ± 5	(5.2)	(2.0)	(185)
$Fe_8Cr_{32}Ti_{60}$	450 ± 5	470 ± 30	43 ± 5	510 ± 5	5.6 ± 0.5	2.3 ± 0.4	109

tending over a period of several hours [(b)]. Concomitantly with the first contraction the resistivity decreases while during the second one it increases [(c)]. A careful inspection of the line positions in the x-ray diffraction patterns only confirmed the initial contraction, however, while the second one apparently leaves the lattice unchanged. Yet even a third process is observed if isothermally preannealed samples are heated to above T_S: the material now expands, by an amount similar to the second contraction, while its resistivity decreases towards its former value. We do not presently understand the nature of the two last-mentioned processes and will ignore them in the following discussion.

A tempting interpretation of the enthalpy reaction is to view it as the vitrification proper, i.e., as the thermodynamic transition from the undercooled β solid solution to a more stable amorphous solution. The latter would be expected to show a glass transition, fully in line with the specific-heat reaction as observed. Additional evidence supporting this view will be given below. The only problem is that x-ray diffraction (Fig. 5) of the "glass"

resulting from the enthalpy reaction clearly shows crystalline long-range order [(b)], although subtly different from the as-quenched β structure. That is, it can be inferred from the increase of linewidth that the resulting structure is more disordered.[14] Only after prolonged annealing at temperatures above T_S does progressive amorphization—in competition with equilibrium phase formation—occur near the surface [(c)]. No enthalpy effects are detectable during amorphization, and the steps remain unchanged as well. This means that the long-range-ordered phase resulting from the enthalpy reaction and the amorphous phase growing above T_S are, to a first approximation, the same thermodynamic phase.

On the other hand, there is a rather strong expansion as well as an increase in resistivity associated with the amorphization process above T_S. Attempts to obtain
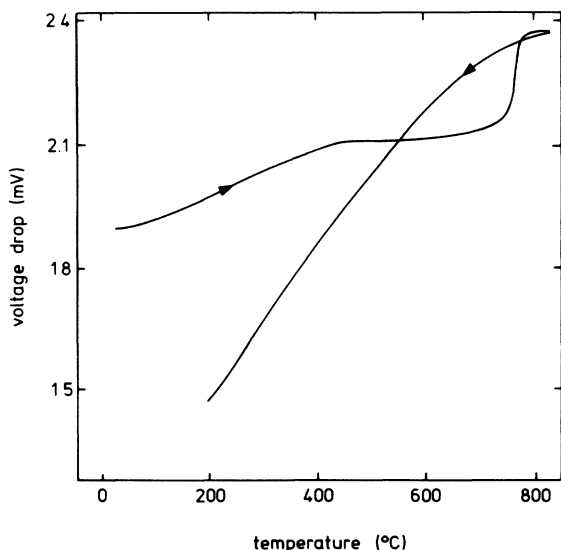

FIG. 3. Voltage drop vs temperature for a freshly prepared β-$Cr_{40}Ti_{60}$ rod fed with a constant current. The curve is proportional to the resistivity; its slope gives the TCR.

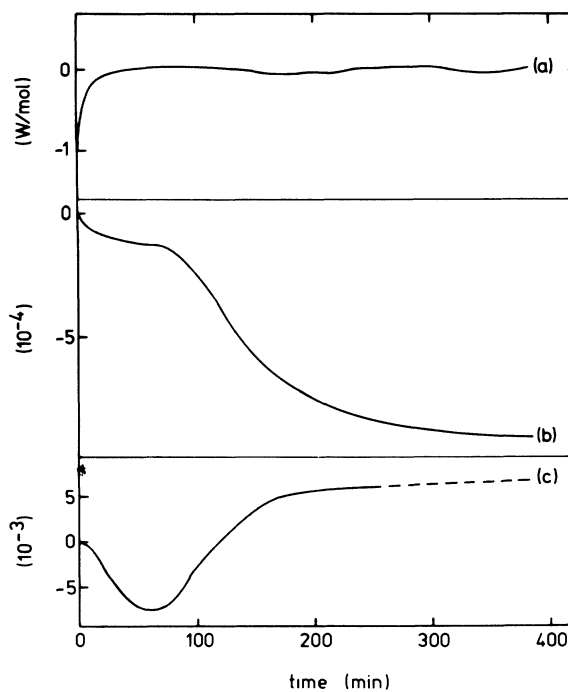FIG. 4. Isothermal measurements of β-$Cr_{40}Ti_{60}$ rods at 440 °C. (a) DSC signal; (b) relative dilatometer signal; (c) relative voltage drop.

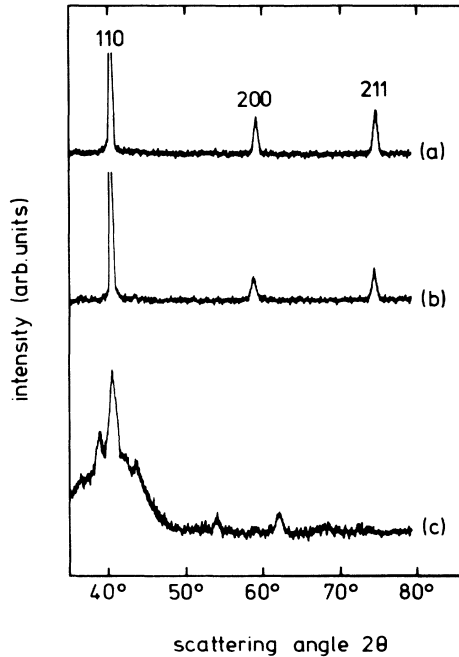FIG. 5. X-ray diffraction patterns of a $Cr_{40}Ti_{60}$ sample at room temperature. (a) The as-quenched β phase; (b) after the enthalpy reaction; (c) after repeated cycling between room temperature and 600 °C.

quantitative values for these quantities unfortunately failed because complete amorphization of entire rods could not be achieved. At temperatures close to T_S amorphization is too slow compared to instrumental drift, while at higher temperatures partial equilibrium phase formation could not be suppressed. The volume increase most probably poses severe kinetic constraints on bulk amorphization, and may also explain why the process always starts at the surface or at grain boundaries[5] and seems to slow down thereafter. We shall in the following concentrate on the events that precede structural amorphization (for a documentation on the latter we refer to Refs. 5 and 11).

In summary, then, the above experiments have established the occurrence of two microscopically relevant transitions associated with spontaneous vitrification: an irreversible exothermic reaction involving a decrease in volume as well as a change in electrical behavior, and a reversible transition involving steplike changes in specific heat and thermal expansion coefficient. Amorphization does not occur if either of these effects is missing, as in the case of $Cr_{20}Ti_{80}$ (Table I) or splat-cooled samples (Ref. 15).

IV. DISCUSSION

A. The specific heat reaction

At room temperature the specific heat is close to the classical value $3R$ (where R is the gas constant), indicating that all vibrational modes are activated. An explanation of the specific heat and thermal expansion anomalies at T_S in terms of a thermodynamic order-disorder transi-

tion appears improbable for the following reasons: (i) the specific heat and thermal expansion coefficient curves are steplike rather than λ-shaped; (ii) the occurrence and height of the steps depends on the presence of defects rather than on composition, suggesting a structural rather than chemical origin (see below); (iii) no effect on resistivity is observed near T_S. Hence, we view the additional, discontinuous increase of the specific heat by more than $R/2$ at T_S as the unfreezing of some new, nonvibrational degree of freedom. Such large steps in specific heat above the Debye temperature caused by kinetic effects have not yet been observed with crystalline solids to our knowledge. On the other hand, they are typical for glass transitions.

A priori, there is nothing fundamental forbidding a "glass transition" in a real crystal. The glass transition in melt-quenched glasses is usually ascribed to the unfreezing of some kind of "holes"—modeled as free volume or as various sorts of defects.[16-18] Their unfreezing causes a strong increase of the atomic mobility, which then enables configurational relaxation. It must be pointed out that in β-Cr-Ti alloys the specific-heat transition as well as vitrification is only observed in the presence of "holes." Splat-cooled samples of $Cr_{40}Ti_{60}$ do not show the specific-heat reaction, nor do they vitrify. Only after the introduction of point defects by light-ion irradiation do such samples behave in the manner expected.[15] It is important to emphasize, however, that atomic long-range diffusion is generally not required for spontaneous vitrification, since it is a polymorphous transition. It is apparently sufficient when defects diffuse and thereby provide to the atoms the short-range mobility required for structural relaxation.

Recognizing the specific-heat reaction as a kinetic effect, we can apply a dynamic analysis to the data as follows. The total observed specific heat $dH(T,t)/dT$ is separated into a static term $(\partial H/\partial T)_t$ (which equals $3R$ at room temperature) and a dynamic relaxation term $(\partial H/\partial T)_T = \delta H/\tau$:

$$dH(T,t)/dT = (\partial H/\partial T)_t + \delta H/(\tau r) , \tag{2}$$

where $r = \partial T/\partial t$ is the heating rate. Assuming a thermally activated relaxation time of the form $\tau \sim \exp(-h/RT)$, the following approximation can be derived near T_S:[19]

$$d \ln(r)/d(1/T_S) \approx -h/R . \tag{3}$$

Figure 6 is a logarithmic plot of heating rate versus $1000/T_S$ for $Cr_{40}Ti_{60}$. From this plot an activation enthalpy h of 3.1 ± 0.3 eV is derived. This value is typical for glass transitions in metallic glasses.[19,20]

In summary, we interpret the specific-heat reaction as a kinetic transition related to the unfreezing of mobility. The newly acquired mobility enables structural relaxation, which—for certain compositions—takes on the form of amorphization.
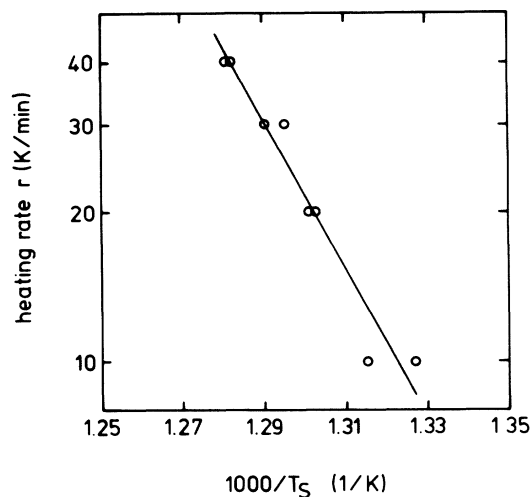
FIG. 6. Logarithmic plot of heating rate r vs $1000/T_S$ for a $Cr_{40}Ti_{60}$ sample after the enthalpy reaction. T_S is defined in Fig. 1.

FIG. 7. Logarithmic plot of r/T_H^2 vs $1000/T_H$ for β-$Cr_{40}Ti_{60}$. Open dots are from the calorimeter and the solid square is from the dilatometer. r denotes the heating rate; T_H is defined in Fig. 1.

B. The enthalpy reaction

The enthalpy reaction bears some resemblance to martensitic transformations and relaxations of quenched materials in general. In contrast to normal relaxations, however, the enthalpy reaction is associated with a slight structural disordering rather than ordering, and the reaction enthalpy decreases, rather than increases with increasing cooling rate. The following observations characterize the reaction.

(i) The long-range order and chemical homogeneity of the material is preserved during the reaction, indicating that no long-range diffusion is involved.

(ii) The enthalpy change associated with the transition is relatively small, of an order typical for displacive transitions. In particular, it is comparable to the reaction enthalpies of martensitic transitions[21] or of irreversible, polymorphous relaxations in metallic glasses.[22]

(iii) The reaction is thermally activated. An activation energy can be determined from the variation of T_H (temperature of maximum transformation rate) with the heating rate r.[23] From Fig. 7, which is a logarithmic plot of r/T_H^2 versus $1000/T_H$ for β-$Cr_{40}Ti_{60}$, an activation energy of 2.0 ± 0.3 eV is deduced. Activation energies of the same order are observed in metallic glasses during irreversible relaxations below the glass temperature[24] or during polymorphous crystallization.[25]

(iv) The sound velocity decreases markedly during this transition.[5,7] The sound velocity is related through the elastic moduli to the elastic (size-mismatch) energy stored in the material.[4,26] Its decrease indicates that the residual stress which arises in the β phase because differently sized atoms are packed on a single coherent lattice, is lowered by atomic displacements. It was recently proposed that highly stressed solid solutions may stabilize even by assuming an amorphous structure through such a mechanism.[27] Such a reaction would show both an enthalpy and a volume effect, as observed.

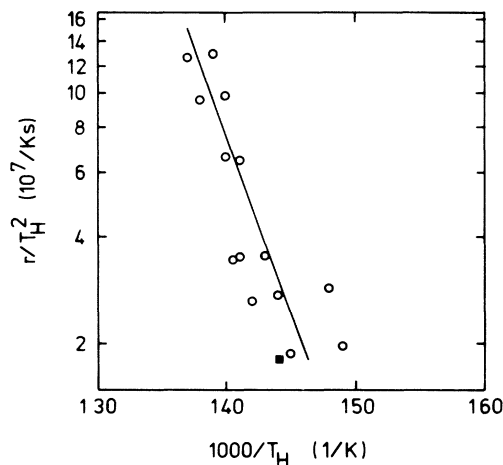The cited evidence suggests that the enthalpy reaction

is driven by an elastic excess energy, and occurs through thermally activated atom displacements of the order of an atomic distance. This implies a relation between the size-mismatch energy and the reaction enthalpy. In fact, their concentration dependences are similar, as both increase towards the equiatomic composition. The reaction enthalpy can thus be viewed as a measure for the topological instability of the quenched β phase. From the thermodynamic point of view, the size-mismatch energy results in a range of chemical spinodal instability.[28] Indeed, thermodynamic modeling of the Cr-Ti β phase based on accepted data[29] predicts spinodal instability at T_H for concentrations larger than 20 $at.\ \%$ Cr, i.e., just for those that show the enthalpy reaction and eventual amorphization.

The present data thus support the earlier conclusion that the enthalpy reaction is driven by the elastic excess energy which further destabilizes the marginally stable bcc lattice.[3] Perhaps even more significant is the realization that the resulting structure is able to undergo polymorphous amorphization without a further thermodynamic transition. Thermodynamically this means it is a liquid or a glass, albeit a crystalline one.

C. Modeling

How can the interpretation of the enthalpy reaction as the transition from the β to the liquid be reconciled with the undeniable crystallinity of the latter? By the simple realization that the transition occurs below the glass transition, i.e., in a temperature range characterized by nonergodic behavior.[30] Rather than having access to its full configurational phase space, the system remains locked in its particular microstate, and this in our case happens to be bcc-like. In simpler terms, in this state of the material there is no longer any restoring force stabilizing the bcc lattice, but there is no atomic mobility to change the configuration either. Only when heated into the ergodic regime above T_S is there sufficient mobility

for configurational sampling, which leads to progressive amorphization.

We have already pointed out the relationship between the enthalpy reaction and martensitic transformations. In fact, a mechanistic approach to understand vitrification is to view the enthalpy reaction as a disturbed martensitic transformation. "Disturbed" in this context means that the parent crystal contains a high density of defects by which the correlation between the motions of individual atoms, essential for martensitic transformations, is broken with the result of disordering. In the extreme case this may, as postulated by Dubois,[31] result in amorphization. In the present case the condition for "martensitic" instability is approached before true amorphization becomes kinetically possible. Experimental evidence linking vitrification to martensitic transformation also exists for ZrCu (Ref. 32) as well as for ion-beam-irradiated Al-Ni (Ref. 33) and Zr_3Al.[34]

A more general thermodynamic approach towards solid-state amorphization is the concept of low-temperature melting, in which the amorphous phase is considered an extension of the liquid.[35] Applied to the present case this requires the free energy versus temperature curves of the liquid and the β phase to intersect twice. To make this possible, the entropy of the liquid must decrease strongly enough on undercooling to become lower than that of the β phase. This would be conceivable if the undercooled liquid (and the glass as well), as opposed to the β phase, was chemically ordered.[36] In contrast to usual melting where ΔS, ΔH, and ΔV are positive, negative values of ΔH and ΔS should come out on vitrification of the β phase. The name "inverse melting" was proposed for this reaction.[36] The observed transformation at T_H can indeed be regarded as inverse melting: It is exothermic, and there is a volume contraction. Further, there is evidence for chemical order implying a decrease of entropy as well.[37]

V. SUMMARY AND CONCLUSIONS

We have found that the spontaneous vitrification of Cr-Ti and Cr-Ti-Fe alloys involves a sequence of events well separated from each other with respect to time and temperature. The microscopically relevant ones are the following.

(i) A nondiffusive transition into an intermediate state is observed at a temperature between 390 and 490 °C, depending on composition. The transformation can be understood as "inverse melting," i.e., the thermodynamic transition from the quenched β phase into the frozen liquid, even though the resulting phase exhibits configurational long-range order.

(ii) At a slightly higher temperature all samples undergo a kinetic transition where the mobility required for configurational relaxation unfreezes. This transition manifests itself by large and reversible steps in the specific heat and the coefficient of thermal expansion, in close resemblance to glass transitions.

(iii) Progressive structural amorphization then occurs at temperatures above reaction (ii) in those samples that have undergone both reactions (i) and (ii). The expansion associated with amorphization probably inhibits catastrophic transformation and limits a thorough vitrification of the bulk.

Probably the most prominent finding of the present work is the occurrence of an intermediate state (resulting from the enthalpy reaction) which combines thermodynamic properties of a supecooled liquid or a glass in the vicinity of the glass transition with the translational invariance of a crystal. Being configurationally frozen, this "crystalline glass," as we call it, is constrained to retain the structure of its parent state (β phase)—exactly as a melt-quenched glass is constrained to retain the structure of the liquid. Only when mobility is provided by heating above the "glass transition" does the frozen structure relax, so to speak, into its amorphous configuration.

ACKNOWLEDGMENTS

[1] S. M. Shapiro, in Competing Interactions and Microclusters: Statics and Dynamics, Vol. 27 of Springer Proceedings in Physics, edited by R. Lesar, A. Bishop, and R. Heffner (Springer-Verlag, New York, 1988), p. 84.

[2] C. Zener, Elasticity and Anelasticity of Metals (University of Chicago Press, Chicago, 1948).

[3] A. Blatter and M. von Allmen, Phys. Rev. Lett. 54, 2103 (1985).

[4] M. von Allmen and A. Blatter, Appl. Phys. Lett. 50, 1873 (1987).

[5] A. Blatter, N. Blatzer, and M. von Allmen, J. Appl. Phys. 62, 276 (1987).

[6] A. Blatter and M. von Allmen, Mater. Sci. Eng. 97, 93 (1988).

[7] A. Blatter, N. Koch, and U. Kambli, J. Less-Common Met. 145, 81 (1988).

[8] This suggests that the observed values have to be considered as lower bounds, to be used for comparing different composi-tions. Apparently part of the reaction already occurs during the quench. For water-quenched samples ΔH was found to be 50% larger than for copper-quenched ones.

[9] R. F. S. Hearmon, in Landoldt-Börnstein, New Series III/11, edited by K. H. Hellwege (Springer, Berlin, 1979), p. 20.

[10] R. L. Fleischer, R. S. Gilmore, and R. J. Zabala, J. Appl. Phys. 64, 2964 (1988).

[11] A. Blatter, J. Gfeller, and M. von Allmen, J. Less-Common Met. 140, 317 (1988).

[12] J. Gfeller, A. Blatter, and U. Kambli, J. Less-Common Met. 157, 223 (1990).

[13] J. H. Mooij, Phys. Status Solidi A 17, 521 (1973).

[14] The structural differences are planned to be analyzed in detail in a forthcoming publication.

[15] A. Blatter, U. Kambli, Ch. Wirz, R. Giovanoli, K. Dyrbye, and J. Bottiger, Phys. Rev. B 40, 12 503 (1989).

[16] M. H. Cohen and G. S. Grest, Phys. Rev. B 20, 1077 (1979).

[17]W. Kauzmann, Chem. Rev. **43**, 219 (1948).

[18]D. Srolovitz, V. Vitek, and T. Egami, Acta Mettal. **31**, 335 (1983).

[19]C. T. Moynihan, A. J. Easteal, J. Wilder, and J. Tucker, J. Phys. Chem. **78**, 2673 (1974).

[20]H. Baxi and T. B. Massalski, Mater. Sci. Eng. **97**, 291 (1988).

[21]A. Planes, R. Romers, and M. Ahles, Scr. Metall. **23**, 989 (1989).

[22]Z. Altounian, Mater. Sci. Eng. **97**, 461 (1988).

[23]D. W. Henderson, J. Non-Cryst. Solids **30**, 301 (1979).

[24]E. Kokmeijer, E. Huizer, B. J. Thijsse, and A. van den Beukel, Mater. Sci. Eng. **97**, 505 (1988).

[25]U. Köster and U. Herold, in *Glassy Metals I,* edited by H.-J. Güntherodt, and H. Beck (Springer-Verlag, Berlin, 1981), p. 225.

[26]A. K. Niessen and A. R. Miedema, Ber. Bunsenges. Phys. Chem. **87**, 717 (1983).

[27]Y. T. Cheng and W. L. Johnson, Science **235**, 997 (1987).

[28]The coherent spinodal is not known, but in the partially disordered β crystal it might not be too far from the chemical one.

[29]J. L. Murray, *Phase Diagrams of Binary Titanium Alloys* (American Society for Metals International, Metals Park, Ohio, 1987), p. 68.

[30]J. Jäckle, Philos. Mag. B **44**, 533 (1981).

[31]J.-M. Dubois, J. Less-Common Met. **145**, 309 (1988).

[32]A. W. Nicholls, I. R. Harris, and W. Mangen, J. Mater. Sci. Lett. **5**, 217 (1985).

[33]C. Jaouen, M. O. Ruault, H. Bernas, J. P. Rivière, and J. Delafond, Europhys. Lett. **4**, 1031 (1987).

[34]L. E. Rehn, P. R. Okamoto, J. Pearson, R. Bhadra, and M. Grimsdicht, Phys. Rev. Lett. **59**, 2987 (1987); P. R. Okamoto, L. E. Rehn, J. Pearson, R. Bhadra, and M. Grimsdicht, J. Less-Common Met. **140**, 231 (1988).

[35]W. L. Johnson, Prog. Mat. Sci. **30**, 81 (1986).

[36]A. L. Greer, J. Less-Common Met. **140**, 327 (1988).

[37]Short-range order in glassy Cr-Ti thin films was recently established with resistivity measurements (see Ref. 12). Preliminary results from neutron diffractometry indicate that chemical short-range ordering precedes amorphization in undercooled β phases.
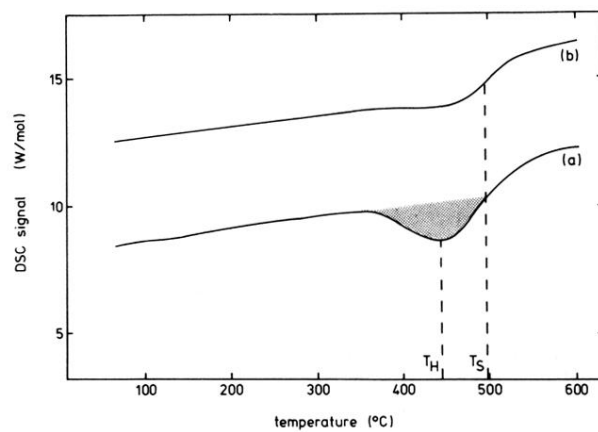
FIG. 1. DSC signal vs temperature curves for β-$Cr_{40}Ti_{60}$ obtained at a heating rate of 20 K/min. Trace (a) is from the first and trace (b) from the second heating cycle. (b) has been shifted upwards for the sake of clarity. During the first cycle an exothermic reaction with enthalpy ΔH (shaded area) occurs near T_H. At temperature T_S there is a reversible step.
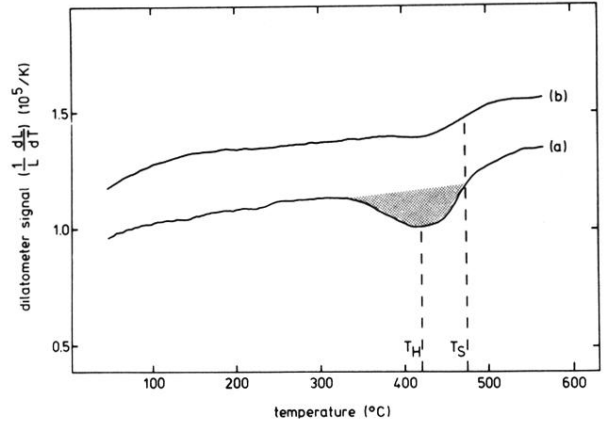
FIG. 2. Dilatometer signal $(1/L)\,(dL/dT)$ vs temperature curves, analogous to Fig. 1 but with a heating rate of 5 K/min. The shaded area corresponds to a volume contraction ΔV.